Nanotechnology Perceptions
ISSN 1660-6795
www.nano-*ntp.com*

Scaling Exponents In Electronic Growth Mechanism

Dr. Arindam Pal

Department of Physics, Yogoda Satsanga Palpara Mahavidyalaya, Palpara, Purba Medinipur – 721458, India.

We have studied the growth dynamics in the electronic growth of Ag on Si(111)-(7×7) surfaces for a film thickness ranging from 1-80 monolayers. The scaling exponents □□□□ and 1/z are determined using scanning tunneling microscopy. Ag films exhibit growth of flat-top plateaus of preferential heights due to an electronic growth mechanism. We have observed□□ = 0.66 ± 0.02 at the early stage of the electronic growth with two atomic layer height flat-top isolated Ag mounds formation. However, □ increases to 0.75 ± 0.04 at the later stage of the growth when isolated mounds coalesce and form percolated structures maintaining preferential heights of an even number of atomic layers and finally 0.86 ± 0.03 in the Ag mounds. Interface width w increases as a power law of coverage (□), $W \sim q^{b}$, with growth exponent □ = 0.34 ± 0.01 and lateral correlation length □ grows as $\xi \sim \theta^{1/z}$ with 1/z = 0.34 ± 0.05.

Keyword: Electronic growth, Height-height Correlation Function, Growth Exponents Interface width.

Introduction

The study of metal-semiconductor interfaces has been a topic of significant interest for decades due to their technological importance. Considerable efforts have been devoted to controlling their electronic properties and developing films with atomically smooth growth fronts and interfaces, which play a crucial role in microelectronic devices. In this regard, the Ag/Si(111) system is one of the most extensively studied because it is a non-reactive metal-semiconductor system.[1, 2] Nevertheless, growth morphology of Ag film has been found to depend on the deposition rate and growth temperature.[3-5] Recently, "electronic growth" mode was proposed for growing metal over-layer on semiconductor substrates.[6] In metal films, conduction electrons are restricted by the metal surface on one side and the metal-semiconductor interface on the other. This confinement leads to the formation of quantum well states by the free electrons in the metal, which, in turn, contribute to stabilizing the film's thickness.[7, 8] As an example, a critical thickness of the films is proposed beyond which atomically flat Ag films can be grown on GaAs(111) substrate[9]. Electronic growth mode is observed in case of Ag film grown on Si(111)-(7×7) surfaces. At low temperature growth of Ag on a Si(111)-(7×7) reconstructed surface, followed by room temperature annealing, produce 3D plateau-like Ag islands with strongly preferred height of two atomic layers on a wetting layer.[7] The islands increase the number density and lateral extension with coverage with no change in height and

eventually form a percolated network type growth. Recently, we have reported the growth of Ag nanostructures at room temperature on Si(111)-(7×7) surfaces over a wide range of film thickness that shows plateau-like percolated Ag islands with an N-layer (N even) height preference.[10] We have not observed any thickness window within which a smooth Ag film can be grown. Moreover, Ag film becomes rougher while growing. In order to understand the kinetics of this roughening, we examined the roughness evaluation of the Ag growth front with coverage. An instability in film growth is observed, resulting from a linear diffusion process in which the local surface slope remains constant over time. The findings in this study demonstrate a competition between kinetic roughening, driven by linear diffusion, and the electron confinement effect within the film, which together influence the evolution of surface morphology. While increased lateral growth promotes the formation of a smoother film, the linear diffusion process counteracts this effect, leading to surface roughness.

Experimental Details

Ag growth and scanning tunneling microscopy (STM) measurements were performed in a custom made molecular beam epitaxy (MBE) chamber coupled with an ultra high vacuum (UHV) variable temperature scanning tunneling microscope (VTSTM, Omicron). Base pressure in the growth chamber was 1×10^{-10} mbar. Samples cut from a P-doped n-type Si(111) wafer (oriented within ±0.5°) with resistivity of 10–20 **Ω** cm were introduced in the UHV chamber. Atomically clean, reconstructed Si(111)-(7×7) surfaces were prepared by degassing at about ~ 600°C for 12–14 hours and then flashing briefly at ~ 1250°C to remove the native oxide layer. The substrates were then cooled down to room temperature (RT) and (7×7) surface reconstruction was observed by STM. Ag atoms were evaporated from Knudsen cell made of pyrolytic boron nitride (PBN) and deposited on Si(111)-(7×7) reconstructed surface which was kept at RT. The deposition rate was 2 monolayers/min for all the samples. We have deposited 1, 1.4, 1.6, 1.8, 2, 4, 5, 10, 30, 40 and 80 ML Ag on Si(111)-(7×7) reconstructed surfaces. Here we define 1 monolayer (ML) of Ag is equivalent to the nominal surface atomic density of Ag(111), 1.5×10^{15} atoms/cm^2. The chamber pressure increased to 5×10^{-10} mbar during deposition. Following deposition the samples were transferred to VTSTM chamber for morphology characterization.

Results and Discussions

Figure.1 represent the STM images of Ag films for coverages ranging from 1 to 80 ML. The samples with Ag coverage exhibit plateau-like Ag mound formations on top of a wetting layer of 1ML to 1.8 ML (Figure 1 (a-d)). These mounds have grown laterally with coverage keeping height of the structures constant. As the Ag coverage increases, the mounds merge, forming percolated structures. In the samples with Ag coverage, we observed the development of percolated mound structures that expand both laterally and vertically from 2 to 80 ML as shown in Figure.1 (e-k).

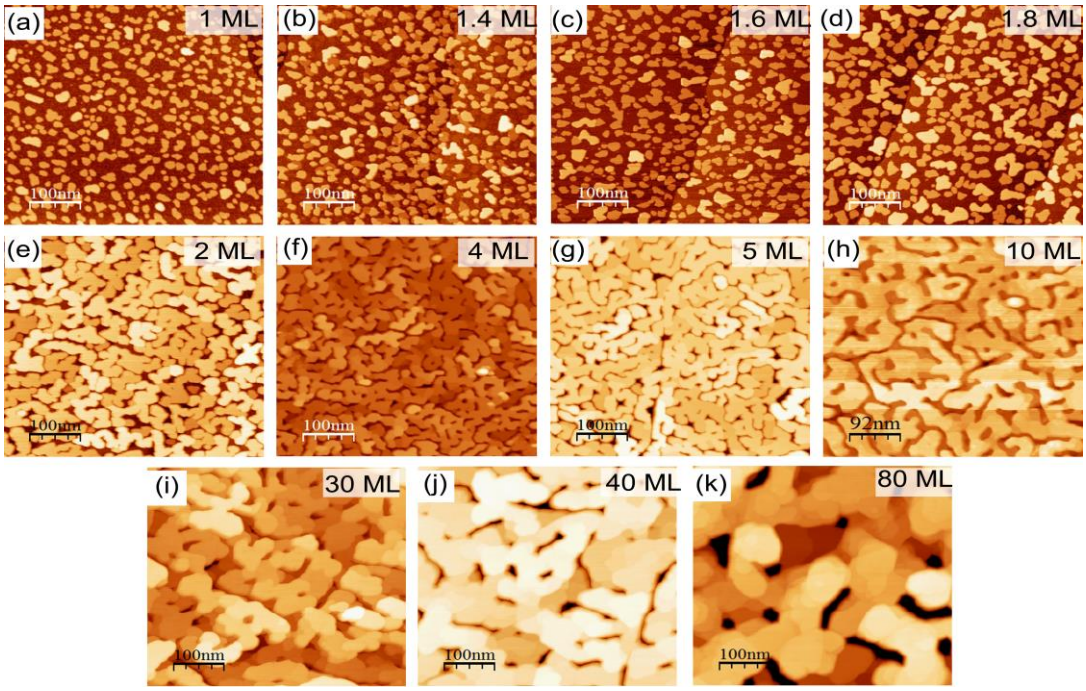

Figure 1 (Color online) STM images of (a-k) Ag/Si(111)-(7×7) surfaces, showing the surface morphology for 1, 1.4, 1.6, 1.8, 2, 4, 5, 10, 30, 40 and 80 ML coverage. All the images are in 500×500 nm^2 area.

A strongly preferred height of two atomic layers is observed for the samples up to 1.8 ML (below percolation). For thicker samples, percolated structures showed a tendency to grow with preference of N-layer height, where N is even (two, four etc.) as reported in ref.10. This preferential height growth of Ag on Si(111)-(7×7) surfaces has been associated with electronic growth modes where, electronic confinement within the metal film plays important role in determining the morphology of the films with magic heights.[7, 10] We have observed the hexagonal flat top island from 30 ML to 80 ML coverage.

To gain insight into the dynamic behavior of the detailed growth processes, we analyze different scaling exponents and the local surface slope. These parameters are derived from the height-height correlation function, G(r,θ), which represents the mean square height difference between two surface points separated by a distance r for a given atomic coverage (□□□as $G(r,q) = \left\langle \left[h(r,q) - h(0,q) \right]^2 \right\rangle$ where h(r,□) and h(0,□) are the heights of the surface at the locations separated by a distance r and the brackets signify an average over pairs of points.[11-14] As the growth rate of Ag is kept constant throughout the experiments, we have considered the dynamic behavior of the growth in terms of □ instead of time t. For the small r, height-height correlation function $G(r,q) = [m(q)\, r]^{2a}$ with r<<□□□□, where, □□□□□is the characteristic in-plane length scale, □□□is the roughness scaling exponent and m(□) is the local slope of the surface profile for small length scale.[13, 15] m(□) is calculated from the fitting

of linear portion of log-log plot of G(r,□) vs r using above equation. The spacing between the mounds is a crucial parameter for characterizing the mound surface, commonly referred to as the wavelength (λ). The lateral correlation length, ξ(θ), represents the distance beyond which surface heights exhibit minimal correlation. For mounded surfaces, it effectively corresponds to the size of the mounds.[16] The wavelength (λ) and lateral correlation length (ξ) are not essentially equal. They only must satisfy the relation $\xi \leq \lambda$ because mounds are separated by at least their size. Only if the mounds grow next to each other would imply that $\xi = \lambda$.[17]

In this study $G^{1/2}$(r,□□) was calculated from STM images for different coverages and is presented in Figure 2. To minimize sampling-induced effects in the G(r,□□), care has been taken to include many AFM images in the averaging of G(r,□□) multiple AFM images were included in the averaging process. Our analysis confirmed that using 6 to 10 AFM images per sample was sufficient to obtain statistically reliable data to obtain G(r,□□) plot. Figure 2(a) show $G^{1/2}$(r,□□) vs r plots for the coverage up to 1.8 ML, corresponding to the growth of two atomic layer preferred height. Figure 2(b) shows the same plot for the coverages 2ML to 30 ML, when mainly percolated structures formed with a tendency of growing preference of even atomic layers. To monitor the roughening process quantitatively, we measure the width w(□) of the interface as function of coverage (□□□□Following the method described in ref.[18, 19], we define the surface roughness amplitude W(□□□(shown by arrow marked in Figure 2 as the value of $G^{1/2}$(r,□□) at the first local maximum, W(□)= $G^{1/2}$(□/2) where □□marked by an upward arrow is the position of r at the first local minimum of $G^{1/2}$(r). This definition of roughness amplitude is preferred over the large r limit of G (r) because artifacts at large length scales can affect STM data. The roughness exponent □□□was determined from a fit to the linear part of the log-log plot of $G^{1/2}$(r) vs r. We have observed two values of roughness exponent □. Below percolation the value of is 0.66 ± 0.02, □ for percolated structures is 0.75 ± 0.04 and 0.86 ± 0.03 in the hexagonal flat top island region as shown in Figure 2.

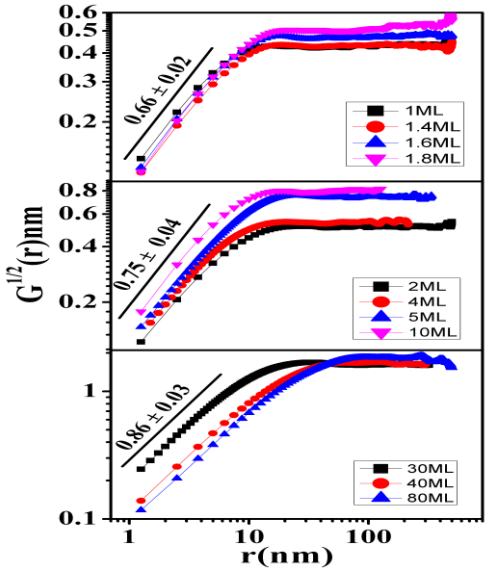

Figure 2 (Color online) Square root of height-height correlation function calculated from STM images of 1 to 80 ML Ag coverages in three different region of Ag coverages. Roughness exponent (α) is calculated from the power fitting of the linear portion.

Roughness width (W), increases as power law of □ as, W(□□□□□□□□□□□□ The exponent □ characterizes the dynamics of the roughening process and is called growth exponent. On the other hand, the lateral correlation length □□□□, increases with □□□as a power law as, □□□□□□□$^{1/z}$, where exponent 1/z is called dynamic exponent. Log-log variation of w versus □ is shown in Figure 3(a) for all the coverages which we explored in this work.

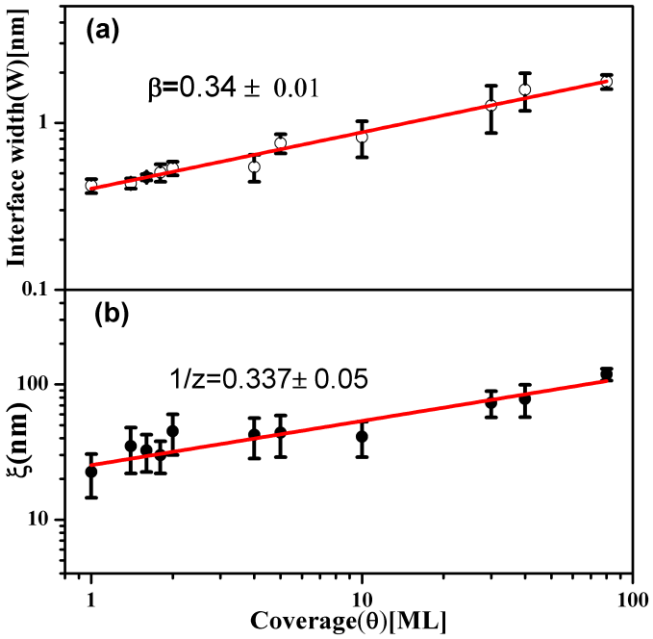

Figure 3 (Color online) Log-log variation of (a) interface width (W) and (b) lateral correlation length (ξ) with coverages (θ). Growth exponent (β) and dynamic exponent (1/z) are calculated from the slope of the α and β curve, respectively.

The growth exponent □ obtained here is 0.34 ± 0.01. The dynamic exponent (1/z) calculated from the log-log plot of □ versus □ as shown in Figure 3(b). The value of 1/z is 0.337± 0.05. Therefore, one can expect to have smooth film growth with faster lateral growth. As predicted in the electronic growth mode, the formation of discrete quantum well states can lead to novel effects including preferred heights and critical thickness of metal films beyond which the film will be atomically flat.[8, 10, 20-22] In case Ag grown on Si(111)-(7×7) surfaces, we have not observed any such critical thickness. Faster lateral growth, as observed, can support the formation of smooth films. However, there is kinetic instability in the growth that does not allow forming smooth films and a roughening in the growth mechanism is observed. A two-step growth mechanism has been popular in which films are grown at low temperature followed by room temperature annealing.[22, 23] At low temperature, a non-equilibrium structure is formed and this drives the system into a metastable state with height preference. However,

it will not be accessible fully if unwanted kinetic processes are enabled. Although the growth of Ag films at room temperature exhibits height preference due to "electronic growth," where quantum well states influence film morphology, kinetic processes are not entirely suppressed. Consequently, roughening is observed, characterized by flat-top mounds at lower coverages and percolated mounds with magic heights at higher coverages. This morphology arises from the competition between quantum well state formation and kinetic growth processes.

From the theoretical treatments of non-equilibrium film growth, the predicted scaling exponents are □=2/3 and □=1/5 if one consider the nonlinear growth equation.[24] However, for the linear growth equation predicts □=1 and □=1/4.[25] On the other hand, due to step edge barrier (Schwoebel barrier), the diffusion can also be limited and form uniformly sized pyramids with stationary slope. The predicted scaling exponents for Schwoebel barrier is □=1 and □=1/4.[26] None of the existing theoretical models account for the exponents observed in the electronic growth mode. This discrepancy leads to instability in electronic growth, causing it to become non-stationary as the local surface slope increases with coverage[12, 13]. n this study, all samples were grown with substrates maintained at room temperature. As a result, the growth kinetics at room temperature contributes to instability in electronic growth. However, the observed growth exponents cannot be explained solely by the diffusion model. The electronic growth mechanism plays a crucial role in shaping the growth front morphology. Consequently, the roughening behavior falls into a distinct universality class that involves both quantum well state formation and local surface diffusion.

Conclusion

In conclusions, we report dynamical scaling exponents for electronic growth of Ag on Si(111)-(7×7) surfaces. The growth front morphology is apparently influenced by the quantum well state formed within the films. However, we have found a roughening mechanism that exists with the electronic growth to control the growth front morphology.

References

1. W. G. Schmidt, F. Bechstedt and G. P. Srivastava, Surf Sci Rep 25 (5-7), 141-223 (1996).
2. E. J. Vanloenen, M. Iwami, R. M. Tromp and J. F. Vanderveen, Surf. Sci. 137 (1), 1-22 (1984).
3. Z. H. Zhang, S. Hasegawa and S. Ino, Phys. Rev. B 55, 9983-9989 (1997).
4. K. R. Roos and M. C. Tringides, Surf. Sci. 302, 37-48 (1994).
5. G. Meyer and K. H. Rieder, Appl. Phys. Lett. 64 (26), 3560-3562 (1994).
6. Z. Y. Zhang, Q. Niu and C. K. Shih, Phys Rev Lett 80 (24), 5381-5384 (1998).
7. L. Gavioli, K. R. Kimberlin, M. C. Tringides, J. F. Wendelken and Z. Y. Zhang, Phys. Rev. Lett. 82 (1), 129-132 (1999).
8. S. J. Tang, C. Y. Lee, C. C. Huang, T. R. Chang, C. M. Cheng, K. D. Tsuei, H. T. Jeng, V. Yeh and T. C. Chiang, Phys Rev Lett 107, 066802 (2011).
9. H. B. Yu, C. S. Jiang, P. Ebert, X. D. Wang, J. M. White, Q. Niu, Z. Y. Zhang and C. K. Shih, Phys Rev Lett 88 (1) (2002).
10. D. K. Goswami, K. Bhattacharjee, B. Satpati, S. Roy, P. V. Satyam and B. N. Dev, Surf. Sci. 601 603–608 (2007).

11.A.-L. Barabási and H. E. Stanley, Fractal Concepts in Surface Growth. (Cambridge University Press, Cambridge, 1995).
12.J. Lapujoulade, Surf. Sci. Reports . 20, 191-249 (1994).
13.M. Pelliccione and T.-M. Lu, Evolution of thin film morphology: modeling and simulation. (Springer-Verlag, New York, 2008).
14.Y. Zhao, G.-C. Wang and T.-M. Lu, Characteriztion of Amorphus and Crystalline Rough Surface: Principles and Application. (Academic Press, London, 2001).
15.J. H. Jeffries, J.-K. Zuo and M. M. Craig, Phys. Rev. Lett. 76, 4931-4934 (1996).
16.M. Pelliccione, T. Karabacak, C. Gaire, G.-C. Wang and T.-M. Lu, Phys. Rev. B. 74, 125420 (2006).
17.J.-K. Zuo and J. F. Wendelken, Phys Rev Lett 78, 2791-2794 (1997).
18.I. J. Lee, M. Yun, S.-M. Lee and J.-Y. Kim, Phys. Rev. B 78, 115427 (2008).
19.D. P. Datta and T. K. Chini, Phys. Rev. B 69, 235313 (2004).
20.H. Liu, Y. F. Zhang, D. Y. Wang, M. H. Pan, J. F. Jia and Q. K. Xue, Surf. Sci. 571 (1-3), 5-11 (2004).
21.L. Huang, S. J. Chey and J. H. Weaver, Surf. Sci. 416 (1-2), L1101-L1106 (1998).
22.A. R. Smith, K. J. Chao, Q. Niu and C. K. Shih, Science 273 (5272), 226-228 (1996).
23.G. Neuhold, L. Bartels, J. J. Paggel and K. Horn, Surf. Sci. 376 (1-3), 1-12 (1997).
24.Z. Lai and S. Das Sarma, Phys Rev Lett 66 (18), 2348-2351 (1991).
25.D. E. Wolf and J. Villain, Europhys Lett 13 (5), 389-394 (1990).
26.M. Siegert and M. Plischke, Phys Rev Lett 73 (11), 1517-1520 (1994).